Journal of Chemical Crystallography
https://doi.org/10.1007/s10870-019-00813-5

ORIGINAL PAPER

β-Chain Hydrogen-Bonding in 4-Hydroxycoumarins

Truc-Vi H. Duong[1] · Todd S. Carroll[1] · Daniel S. Bejan[2] · Edward J. Valente[1]

Received: 17 August 2019 / Accepted: 31 October 2019
© Springer Science+Business Media, LLC, part of Springer Nature 2019

Abstract

In the solid state, some 3-substituted 4-hydroxycoumarins β-ketoester enols form infinite translational hydrogen-bonded β-chains with varying degrees of alignment between adjacent delocalized systems. Nine related structures have been studied. At the strongest, intermolecular associations are polar, purely translation neighbors interact essentially along a 717 pm crystallographic repeat with shortened 260 pm intermolecular $O{\cdot}O_{H\text{-}bond}$ contacts. Four distinctive features characterize these structures: (1) moderately delocalized β-ketoester enol structures, (2) translational misalignment angles between oxygen donors and acceptors less than 10°, (3) buttressing intermolecular C–H·O contacts co-planar with and near the intermolecular O–H·O interactions, and (4) fully extended ketoester enol hydrogen-bond (ap-*anti-anti*) geometries. For non-polar β-chains in related coumarin systems, β-ketoester enol alignments are typically poorer, involve hydrogen-bonding between glide relatives, ap-*syn*-(*anti)* geometry, and the intermolecular $O{\cdot}O_{H\text{-}bond}$ contacts are longer.

Graphic Abstract

Substituted 4-hydroxycoumarins related to phenprocoumon can form well-aligned polar translational β-chains between enolones showing resonance assisted Hydrogen-bonding and a 717 pm repeat along a crystallographic axis.

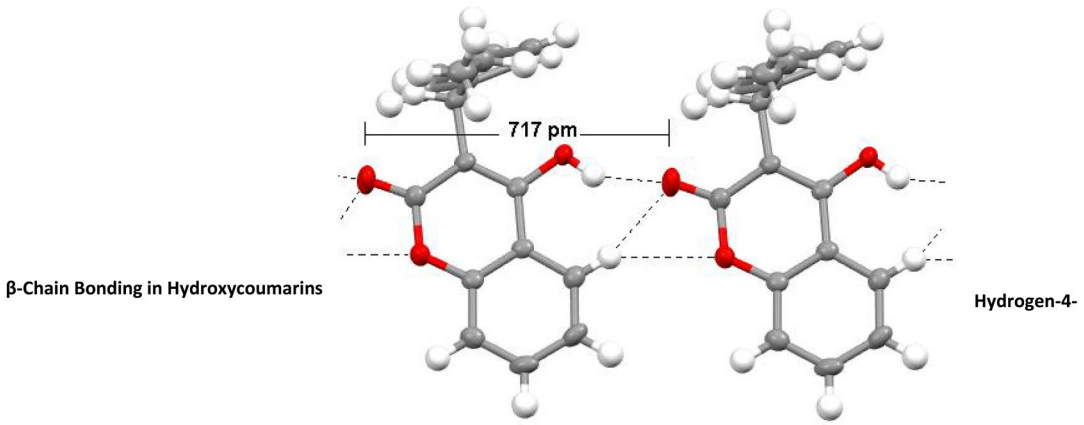

Keywords Hydrogen-bonding · Ketoester enol · Supramolecular · Coumarin · 4-Hydroxycoumarin · β-Chains · Phenprocoumon

Introduction

Stronger hydrogen-bonded assemblies between neutral molecules are often found where the interacting systems are (nearly) coplanar and hydrogen-bonding is cooperative. Thus, carboxylic acids form planar intermolecular complementary hydrogen-bonded dimers, and β-diketone enols

✉ Edward J. Valente
valentee@up.edu

[1] Department of Chemistry, University of Portland, 5000 N. Willamette Blvd., Portland, OR 97203, USA

[2] Science Programs, Washington State University, Vancouver, WA 98686, USA

Published online: 14 November 2019

commonly form rings and homodromous chains linked by hydrogen-bonds [1, 2]. In these neutral O–H·O interactions, the bond angles at H are typically 150–175°, and $O{\cdot}O_{H\text{-bond}}$ distances are less than about 265 pm. Stronger hydrogen-bonding has been called "resonance-assisted" from the alignment of the π-systems and a diminished barrier to proton exchange [3]. Alternative explanations invoke the importance of charge delocalization and the alignment of the adjacent σ-frameworks [4, 5]. There has been some success in gauging the strength of hydrogen-bonding and correlating π-interactions with small differences in the pK_as of the interacting groups [6, 7]. But in β-diketone enols systems with resonance assisted hydrogen-bonding (RAHB), these strategies were typically not applied as the pK_a properties of the donors and acceptors were not readily estimated. In a computational approach to understanding RAHB, a study of bond critical points suggested a covalent character to these interactions especially given the geometric requirements [8]. In contrast, computations have also stressed the importance of electrostatic (dipolar) interactions between π-systems [9].

In an extensive crystallographic study of 5- and 6-ring structures incorporating β-diketone enols and β-ketoester enols, these two neutral classes of hydrogen-bonded systems were found to form chains (β-chains) with stronger $O{\cdot}O_{H\text{-bond}}$ contacts (245–269 pm) [3, 10]. The consistent theme in these supramolecular structures was interactions between translation, screw and glide relatives linking (nearly) coplanar π-systems through an almost linear hydrogen-bonded geometry. In the supramolecular and crystallographic context, translation referred to an interaction between molecules related by "pure translation" and through the translational components of a screw or glide operation. For molecules linked by translation, diketone enols had antiperiplanar (ap) arrangements, and among the 5-ring systems, nearly linear hydrogen-bonding geometry was maintained by a donor *syn* and acceptor *anti* arrangements (Fig. 1). Vertinolide, a substituted cyclopentandione, formed translational β-chains with molecules inclined at about 20° (angle ***a***, Fig. 1), consistent with a more optimal interaction of donor and acceptor oxygens and a 650 pm repeat [11].

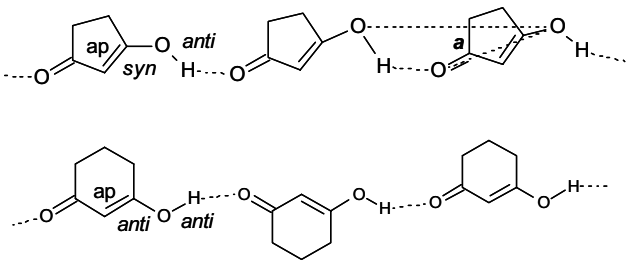

Fig. 1 Cyclopentandiones with ap-*syn-anti* structures show minor misalignments (angle ***a***) between translational relatives. Cyclohexandiones with ap-*anti-anti* structures relate glide relatives

The 6-ring systems (cyclohexandione enols) did not form simple translational β-chains apparently because of intermolecular repulsions [3]. For example, the enol of 2-methyl-1,3-cyclohexandione had ap-*anti-anti* configuration, and formed β-chains linking well-aligned glide relatives (***a***: 4°). A crystallographic axis essentially coincided with the hydrogen-bonding direction and a 685.4 pm repeat between molecules [3, 12]. Among other 6-ring systems, the β-ketoester enol represented by 4-hydroxycoumarins (**1**) may be promising. Unsubstituted 4-hydroxycoumarin crystallizes as a hydrate without forming β-chains and the enol formed hydrogen-bonds with and through its water of crystallization [13]. Some 3-substituted derivatives of 4-hydroxycoumarins however have shown a tendency to form hydrogen-bonded translational or glide β-chains and to adopt ap-*anti-anti* and ap-*syn*-(*anti)* configurations [14–17]. Other 4-hydroxycoumarin derivatives belonging to the dicoumarol family form intramolecular hydrogen-bonded rings between two enolones [18–27]. Dicoumarol enolone systems do not form planar arrangements, and show ordinary weak hydrogen-bonded geometries. Enolones in other 4-hydroxycoumarin derivatives form intramolecular interactions with 3-substituent hydrogen-bond acceptors [28–31].

4-Hydroxycoumarin structures which showed pure translational RAHB include phenprocoumon (marcoumar, **2**) [14, 16]. Both racemic and enantiomeric phenprocoumon form well-aligned β-chains with their enolones. Curiously, these phases are pseudoisomorphorous suggesting the importance of the hydrogen-bonding β-chains in their supramolecular structures. As these types of 4-hydroxycoumarin derivatives have not been examined for the effects of structural alterations on β-chain alignment, this area of interest forms the subject of the present work. Compounds examined include the 3-substitutied 4-hydroxycoumarins (**3**–**11**) related to phenprocoumon, **2** (Fig. 2).

Experimental

Substances were obtained from Sigma-Aldrich Company or TCI America, and used as received. Nuclear magnetic resonance spectra were recorded on Varian or Bruker 400 MHz instruments. Infrared spectra were recorded on a Thermoscientific Smart iTR spectrometer. Melting points were determined on a Stanford Research Systems Digimelt, and are uncorrected. Optical rotation was measured in a 0.25 dm cell on an Optical Activity AA-5. Racemic **2** (mp 179–180 °C) was prepared by the method of Pohl, and resolved with (+)-quinidine giving the (S)-isomer, mp 170–171 °C, lit 170–171 °C [32, 33]. Compounds **3**–**6** were prepared from 4-hydroxycoumarin (**1**) and the appropriate secondary benzylic alcohols or benzyl bromides [34, 35]. After resolving warfarin, the dithioketal of (−)-(S)-warfarin (**8**) was

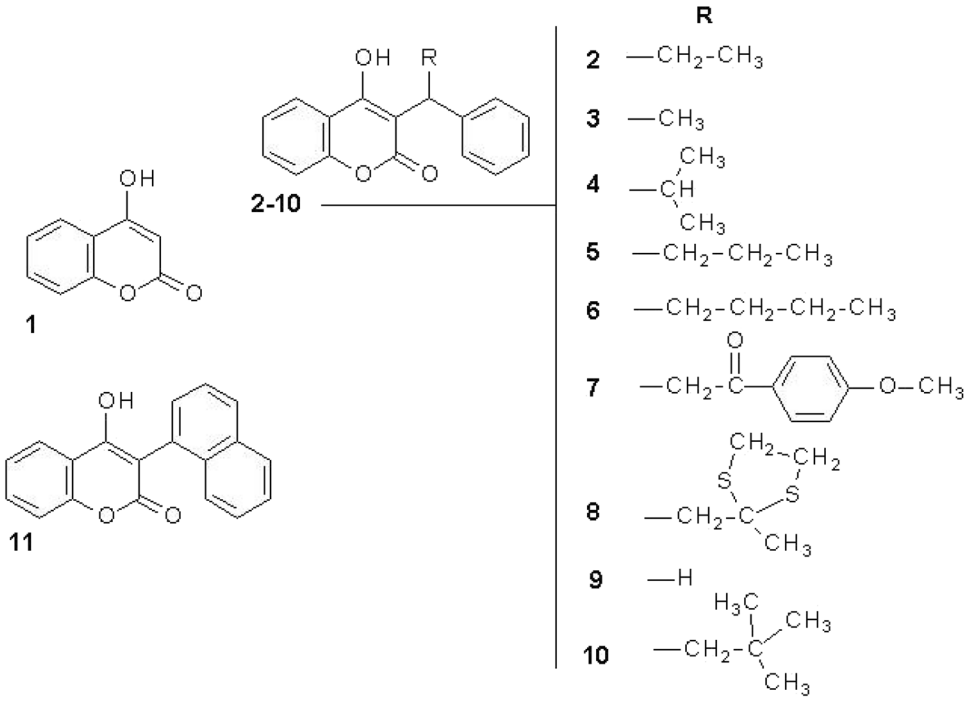

Fig. 2 4-Hydroxycoumarin (**1**) and selected 3-substituted derivatives

prepared, mp 192–193 °C, lit. 193–195 °C [36]. Structural information for compounds (±)-**2**, (±)-**7** and (±)-**11** were taken from the literature [14, 15, 17]. In addition, two more derivatives were prepared to test the structural trends found in the previous group. These include 3-benzyl-4-hydroxycoumarin (**9**) and 3-(1-phenyl-3,3-dimethylbut-1-yl)-4-hydroxycoumarin (**10**). Syntheses of compounds not previously reported or using newer methods are given below.

3-(1-Phenyl-1-ethyl)-4-hydroxycoumarin (3)

To a stirred mixture of 0.162 g **1** (1.00 mmol) and 0.122 g (1.00 mmol) 1-phenyl-1-ethanol in 15 mL nitromethane, 0.050 g (0.22 mmol) of trimethylsilyl trifluoromethanesulfonate was added at room temperature [35]. Successive assays every 20 min during the reaction by thin layer chromatography [SiO_2, $CHCl_3$:EtOAc (10:1)] show the product component (R_f 0.8) no longer increasing after 1 h. The mixture was ended by addition of water, and the aqueous phase made basic with 3 M NaOH and extracted. The nitromethane layer contained unreacted alcohol, which was removed. Acidification of the aqueous phase (3 M HCl) produced a white precipitate which was filtered by suction, and the solid obtained was then washed with two portions of boiling water. 4-Hydroxycoumarin is more soluble in hot water than product **3**. The remaining white solid, 81 mg (30%) and mp 202–204 °C, was recrystallized from acetone:water (9:1). IR (cm^{-1}): 3350, νOH; 1650.8, νC=O; 1607.4, νC=C; ^{1}H-NMR: ($CDCl_3$, 26 °C) δ_H: 7.2–7.7, multiplets, 9H; 6.1, s(br), OH; 4.74, q, 1H, benzyl-H; 1.67, d, 3H, methyl.

Partial resolution of **3**. Racemic **3** (50 mg, 0.18 mmol) was combined with (+)-quinidine (60 mg, 0.18 mmol) in $CHCl_3$, heated briefly to boil, then allowed to cool and then stand at − 10 °C for 12 h. The white precipitate was filtered, and redissolved in $CHCl_3$ with heating, and the cycle repeated twice. This less-soluble salt was partitioned between $CHCl_3$ and 1 N NaOH, and the aqueous phase was then separated and acidified with 3 M HCl. The white solid obtained was levorotatory, and successive recrystallizations did not improve the rotation above an approximate 40% ee; $[\alpha]_D^{25}$ − 65°, c 1.0, 1 M NaOH. Crystals of this possibly eutectic phase, (−)-**3**, were obtained from acetone:water (9:1).

3-(1-Phenyl-2-methylprop-1-yl)-4-hydroxycoumarin (4)

In a sealable reaction tube, 0.162 g **1** (1.00 mmol), 0.172 g (1.00 mmol) *p*-toluenesulfonic acid, and 0.150 g (1.00 mmol) 2-methyl-1-phenyl-1-propanol in 15 mL dichloromethane were combined. To this mixture, 20 mg (0.08 mmol) of $FeCl_3 \cdot 6H_2O$ was added and the tube sealed and heated to 45 °C for 12 h, following a literature method [34, 37]. After cooling, the deep yellow colored mixture was combined with 30 mL water which was then made basic with 3 M NaOH. The organic layer was removed, and the aqueous portion was filtered to remove iron(III) hydroxide. The filtrate was acidified with 3 M HCl to produce a white precipitate. The precipitate was washed with hot water to remove unreacted 4-hydroxycoumarin, and the solid residue

was recrystallized from acetone or ethanol. Yield 0.086 g, 29%, mp 203.6–206.0 °C (decomp.); IR (cm^{-1}): 3233.9, νOH; 1651.9, νC=O; 1606.4, νC=C; ^{1}H-NMR ($CDCl_3$, 25 °C) δ_H: 7.2–7.7, multiplets, 9H; 6.5, s(br), OH; 4.17, d, 1H, benzyl-H; 2.9, m, 1H, C<u>H</u>$(Me)_2$; 1.04, d, 6H, methyls.

3-(1-Phenylbut-1yl)-4-hydroxycoumarin (5)

1-Phenyl-1-bromobutane (1.30 g, 6.1 mmol) and 0.162 g (1.00 mmol) **1** were combined and heated (oil bath) and stirred at 150 °C for 1 h, in a method based on the literature [32]. After cooling, the deep reddish mixture was taken up in 30 mL 1.0 M NaOH and extracted with dichloromethane. The aqueous phase was acidified with 3 M HCl, and the precipitate was filtered and washed with hot water. The white solid obtained was recrystallized from acetone or ethanol, yield 0.118 g (40%), mp 141–142 °C; IR (cm^{-1}): 3341.0 νOH; 1649.7, νC=O; 1602.2, νC=C; ^{1}H-NMR ($CDCl_3$, 25 °C) δ_H: 7.2–7.7, multiplets, 9H; 6.4, s(br), OH; 4.50, t, 1H, benzyl-H; 1.40, m, 2H, C<u>H</u>$_2$; 1.10, t, 3H, methyl.

3-(1-Phenylpent-1yl)-4-hydroxycoumarin (6)

This compound was prepared in a manner similar to that used for **5**. Mp 135.0–136.5 °C; IR (cm^{-1}): 3280.5, νOH; 1653.7, νC=O; 1608.5, νC=C; ^{1}H-NMR ($CDCl_3$, 25 °C) δ_H: 7.2–7.7, multiplets, 9H; 5.9, s(br), 1H, OH: 4.60, t, 1H, benzyl-H; 1.2–1.5, multiplets, 6H, $(C\underline{H}_2)_3$; 0.89, t, 3H, methyl.

3-Benzyl-4-hydroxycoumarin (9)

Compound **9** was prepared by $NaCNBH_3$ reduction of a dicoumarol produced from benzaldehyde and 4-hydroxycoumarin, mp 201–202 °C, lit 201 °C [38, 39]. IR (cm^{-1}): IR (cm^{-1}): 3309.0, νOH; 1655.1, νC=O; 1608.4, νC=C; ^{1}H-NMR: (d_6-DMSO, 25 °C) δ_H: 7.2–7.5, multiplets, 4H, coumarin-H's; 7.28, s, 5H, phenyl-H's; 6.4, s(br), 1H, OH; 5.15, s, 2H, benzyl-H's.

3-(1-Phenyl-2-methylprop-1yl)-4-hydroxycoumarin (10)

This substance was produced using the same method as for **4** but with 1-phenyl-3,3-dimethyl-1-propanol (made by reduction of 3,3-dimethylbutanal with phenyl magnesium bromide). Mp 215.4–216.5 °C; IR (cm^{-1}): 3218.5, νOH; 1671.1, νC=O; 1620.7, νC=C; ^{1}H-NMR ($CDCl_3$, 25 °C) δ_H: 7.66, d,1H, H8; 7.50, t, 1H, H6; 7.38, t, 1H H7; 7.30, d, 1H, H5; 7.26, s, 5H, phenyl; 4.71, t, 1H, benzyl-H; 3.50, s(br), 1H, OH; 2.29, dd, 1H, <u>H</u>–C–H; 2.04, dd, 1H, H–C–<u>H</u>; 1.56, s, 8H, methyls.

Crystallography

Single-crystal X-ray diffraction data were collected on specimens of (−)-**2**, (±)-**3**, (−)-**3**, (±)-**4**, (±)-**5**, (±)-**6**, (−)-**8**, **9**, and (±)-**10** on an Rigaku-Oxford Gemini single-crystal X-ray diffractometer. The assignment of absolute configuration for (−)-**2** and (−)-**8** rests on the known absolute configurations for these phases based on their synthesis and optical rotations [33, 36]. Therefore, it was not necessary to establish configurations by anomalous dispersion, and Mo Kα radiation was used for these structures. The Flack parameter for (−)-**8** was −0.03(9), and provided support that the assigned S configuration is correct. The absolute configuration of (−)-**3** was assigned based on the sign of its optical rotation and a similar application of the resolution method compared to **2**; the Flack parameter for the Cu Kα data set for (−)-**3** was −1.8 (10) consistent with a weak anomalous signal and the partial resolution of the sample (vide infra). It should perhaps be noted that attempted resolution of the homologs with longer alkyl side chains, compounds **4**, **5** and **6**, using (+)-quinidine failed to produce less soluble diastereomeric salts. The structures reported here are of the racemates. Most structures were determined at ambient temperatures, or with a cryojet capable of 101 K as for (±)-**6** and (−)-**2**. The original study on (−)-**2** showed considerable librational freedom, which might have be associated with disorder or a phase change [16]. Relevant experimental details are given in Tables 1, 2 and 3. Intensities were corrected for absorption with an analytical function based on the shape and size of the crystals [40]. Structures were discovered with SHELXS and refined with SHELXL [41]. Metrics on the β-enolone chains were developed in part with MERCURY, and these are given in Table 4 [42].

Models included anisotropic librational parameters for the non-H atoms. Except for hydroxyl H's, positions for H-atoms were calculated and allowed to ride on neighboring atoms together with an isotropic librational parameter set at 120% of the U_{eq} of the neighboring atom, 150% for methyl H's. Enol (O)H-atoms were located in difference fourier maps late in the refinement stages, and the positions were refined while constraining the O–H distances to 0.86 Å according to the usual bias; the H-atom isotropic librational parameter was set to 150% of the U_{iso} of the oxygen. The structure of (−)-**2** was re-determined for this study at room temperature (**2a**) and at 101 K (**2b**). Resolution of **3** could not be pursued beyond the eutectic phase enriched in the (−)-isomer which showed two independent molecules in the asymmetric unit, and each formed β-chains. One chain had well ordered (S)-enantiomers, assigned on the basis of its levorotatory properties in comparison with (S)-(−)-phenprocoumon [33]. The second chain was modeled with overlapped (S) and (R) molecules. Its coumarins were essentially superposed and aligned in the same axial directions, with phenyl

Table 1 Selected crystallographic information for structures (−)-**2a**, **(−)-2b**, **(±)-3**, **(−)-3**

	(−)-**2a**	**(−)-2b**	**(±)-3**	**(−)-3**
Formula	$C_{18}{\cdot}H_{16}{\cdot}O_3$	$C_{18}{\cdot}H_{16}{\cdot}O_3$	$C_{17}{\cdot}H_{14}{\cdot}O_3$	$C_{17}{\cdot}H_{14}{\cdot}O_3$
Formula weight	280.31	280.31	266.30	266.30
Wavelength, pm	71.073	71.073	154.184	154.184
F(000)	592	592	560	560
Size (mm)	0.60, 0.18, 0.15	0.51, 0.24, 0.19	0.31 × 0.07 × 0.06	0.58, 0.21, 0.02
Crystal system	Monoclinic	Monoclinic	Monoclinic	Monoclinic
Space group	P 2_1	P 2_1	P $2_1/a$	P 2_1
Temperature (K)	298 (2)	101 (2)	297 (2)	298 (2)
Cell constants				
a (Å)	7.1717 (4)	7.1400 (4)	7.1953 (7)	7.1639 (5)
b (Å)	17.7827 (10)	17.5868 (9)	24.879 (3)	28.8783 (17)
c (Å)	11.7390 (7)	11.4540 (7)	8.1286 (13)	7.3929 (6)
α (°)	90	90	90	90
β (°)	92.835 (5)	92.017 (6)	112.406 (15)	116.208 (10)
γ (°)	90	90	90	90
Volume ($Å^3$)	1495.27 (15)	1437.38 (14)	1345.2 (3)	1372.2 (8)
Z, density (Mg/m^3)	4, 1.245	4, 1.295	4, 1.315	4, 1.289
μ (mm^{-1})	0.084	0.088	0.728	0.712
Data, R_{merge}	9311, 0.031	8737, 0.055	4945, 0.042	7308, 0.040
Unique data, $I > 2\sigma_I$	6490, 3001	6126, 4083	1683, 1222	4120, 2946
Completeness (%), max. θ (°)	99.8, 30.57	99.8, 30.57	99.6, 55.00	98.9, 61.4
R, wR (unique data)	0.108, 0.104	0.093, 0.144	0.086, 0.166	0.066, 0.116
R ($I > 2\sigma_I$)	0.049	0.066	0.065	0.043
Parameters, restraints	381, 1	381, 1	184, 1	401, 42
Goodness-of-fit	1.001	1.003	1.038	1.014
Δρ(final) ($e^-/Å^3$)	+0.22, −0.14	+0.46, −0.26	+0.19, −0.17	+0.15, −0.13

Estimated standard deviations in parentheses. For (−)-**3**, occupancy factor for (S)-isomer in second chain is 0.215(1) or 0.608 (S)-isomer for the phase; absolute structure parameter − 1.8(10); extinction parameter 0.00165(15)

and methyl groups on the 3-substituent carbon disordered between the two configurations. Constraints were employed during refinement to model overlapping phenyl and methyl groups of the enantiomers, and a partial occupancy factor was included which converged to 0.282 (9) for the minor (R)-enantiomer. Thus, the eutectic crystal composition was 0.718 (9) (S)-isomer. The exact nature of this phase (co-crystal, solid solution, twin) is not known.

Crystals of compound **4** are triclinic but with $a \approx b$ and γ very near 90°; all seven specimens examined showed pseudo-merohedral twinning, multiple domains, and/or non-crystallographic symmetry. For one specimen, reported here, the structure was affected by non-crystallographic symmetry only, and the two components could be modeled: four molecules comprising the asymmetric unit with major occupancy 0.836 (6), and with the minor component of the same atoms shifted by exactly (½ + x, y, z). The shifted structure was included with atom positions and U_{ij}s fixed, and adjusted after every few cycles refining the major atom positions and U_{ij}s. The model converged satisfactorily while other models required restraints, or had lower resolution. For compound **6**, the butyl side chain is disordered over *gauche* and *anti* chain conformations at room temperature (**6b**), with the major conformer (*gauche*) refined with an occupancy of 0.564 (11) for the terminal methyl group; at 101 K, the *gauche* butyl chain is ordered (**6a**). For compound **8**, the model included disordered ethylene links between dithiolan sulfurs. These were refined with partial occupancy factors which refined to 0.52 (3) and 0.65 (3) for the two independent molecules in the asymmetric unit. For compound **10**, the dimethylpropyl side chain appeared disordered but the structure refined for the major enantiomer at 0.843 (4) occupancy with the complement representing the opposite enantiomer occupying the same location. Crystallographic information for the structures (**2a**, 1038546; **2b**,1038547; **(±)-3**, 1946868; **(−)-3**, 1946872; **4**, 1946869; **5**, 1038548; **6a**, 1946871; **6b**, 1039116; **8**, 1038545; **9**, 1946873; **10**, 1946870) have been deposited with the Cambridge Crystallographic Data Center. CCDC data can be obtained from the Cambridge

Table 2 Relevant crystallographic information for structures (±)-**4**, (±)-**5**, (±)-**6a**

	(±)-4	(±)-5	(±)-6a
Formula	$C_{19}{\cdot}H_{18}{\cdot}O_3$	$C_{19}{\cdot}H_{18}{\cdot}O_3$	$C_{20}{\cdot}H_{20}{\cdot}O_3$
Formula weight	294.34	294.34	308.38
Wavelength, pm	154.184	154.184	71.073
F(000)	1248	624	656
Size (mm)	0.30, 0.27, 0.065	0.25, 0.20, 0.06	0.50, 0.15, 0.05
Crystal system	Triclinic	Monoclinic	Monoclinic
Space group	P -1	P $2_1/c$	P $2_1/c$
Temperature (K)	297 (2)	298 (2)	101 (2)
Cell constants			
a (Å)	14.0211 (4)	8.9658 (2)	8.7908 (6)
b (Å)	14.2240 (3)	15.0854 (3)	15.5548 (8)
c (Å)	16.2128 (5)	12.2266 (3)	12.3554 (11)
α (°)	77.010 (2)	90	90
β (°)	77.467 (2)	106.939 (3)	107.965 (8)
γ (°)	89.999 (2)	90	90
Volume ($Å^3$)	3071.55 (14)	1581.94 (6)	1607.1 (2)
Z, density (Mg/m^3)	8, 1.273	4, 1.236	4, 1.275
μ (mm^{-1})	0.685	0.665	0.085
Data, R_{merge}	10566, 0.016	5999, 0.017	13718, 0.056
Unique data, $I > 2\sigma_I$	7458, 6699	2847, 2434	3232, 2390
Completeness (%), max. θ (°)	99.8, 56.2	98.8, 67.9	99.8, 26.2
R, wR (unique data)	0.079, 0.171	0.043, 0.113	0.072, 0.128
R ($I > 2\sigma_I$)	0.074	0.038	0.048
Parameters, restraints	1594, 0	200, 0	209, 0
Goodness-of-fit	1.118	1.043	1.064
Δρ(final) ($e^-/Å^3$)	+0.31, −0.29	+0.14, −0.14	+0.24, −0.22

Estimated standard deviations in parentheses. For (±)-**4**, major component: 0.836 (6); balance fixed and translated by ½ + x., y, z

Crystallographic Data Centre, 12 Union Road, Cambridge CB2 1EZ, UK; fax: +44 1223 336033).

Discussion

To compare the alignment and dimensional features of the β-chains in 4-hydroxycoumarin structures related to phenprocoumon (**2**), several descriptors and measurements are useful (Fig. 3). Enolone ene configurations are generally antiperiplanar (ap). In the hydrogen-bonding between enolones, the donor H-atoms can be *syn* or *anti* within the donor system, and *syn* or *anti* with respect to the acceptor oxygen according to the interaction geometry. In (±)-**2** for example, the configuration is ap-*anti*-*anti*. Neighboring donor and acceptor oxygens may deviate from co-linearity by molecular displacement forming angle **a**. The nearly planar β-ketoester enols may be rotated from a common (coumarin) plane through pitch angle **b**, roll angle **b′**, and yaw angle **b″**. Clearly, the pitch and roll angles **b, b′** may not be large for effective intermolecular π-system (RAHB) congruence. Between hydrogen-bond donor and acceptor atoms, the extent of misalignment of β-chain relatives can also be described by the distance **d** of the acceptor oxygen from the plane of the donor β-ketoester enol π-system. In simple translational β-chains with one molecule comprising the repeat, the angles (**b**, **b′**, **b″**) are all zero necessarily. Alignments can be degraded where the demands of packing and other intermolecular interactions occur and possibly also where glide planes (or screw axes) operate along the interaction direction.

A useful descriptor correlated with the degree of delocalization within a ketoester enol fragment was the sum of the differences between the terminal and internal enolone bond lengths (**Q**). For typical diketone/enol delocalization absent hydrogen-bonding, **Q** took values near ± 20 pm (range − 32 to + 32 pm) [3, 43]. Smaller **Q** values indicated less bond-length disparity and therefore greater π-delocalization. The strength of inter- and intramolecular hydrogen-bonding correlated with the degree of delocalization. Applying these criteria to the β-enolone structure of the cyclopentandione enol vertinolide, translation-relatives were well aligned but

Table 3 Relevant crystallographic information for structures (±)-**6b**, (−)-**8**, **9** and (±)-**10**

	(±)-6b	(−)-8	9	(±)-10
Formula	$C_{20}{\cdot}H_{20}{\cdot}O_3$	$C_{21}{\cdot}H_{20}{\cdot}S_2\,O_3$	$C_{16}{\cdot}H_{12}{\cdot}O_3$	$C_{21}{\cdot}H_{22}{\cdot}O_3$
Formula weight	308.36	384.52	252.27	322.40
Wavelength, pm	154.184	71.073	154.184	154.184
F(000)	656	404	528	344
Size (mm)	0.50, 0.15, 0.05	0.10, 0.10, 0.10	0.44, 0.12, 0.050	0.56, 0.21, 0.10
Crystal system	Monoclinic	Triclinic	Monoclinic	Triclinic
Space group	P $2_1/c$	P 1	P $2_1/c$	P -1
Temperature (K)	297 (2)	297 (2)	298 (2)	298 (2)
Cell constants				
a (Å)	9.0508 (5)	7.1587 (3)	11.7799 (9)	7.1717 (4)
b (Å)	15.8790 (17)	10.9988 (5)	8.3091 (4)	10.0712 (10)
c (Å)	12.2427 (12)	12.2591 (7)	13.0819 (7)	12.8495 (12)
α (°)	90	89.054 (4)	90	84.958 (8)
β (°)	105.746 (14)	83.483 (4)	106.701 (7)	80.588 (6)
γ (°)	90	81.982 (4)	90	84.575 (6)
Volume ($Å^3$)	1693.5 (4)	949.63 (8)	1226.46 (13)	909.00 (13)
Z, density (Mg/m^3)	4, 1.209	2, 1.345	4, 1.366	2, 1.178
μ (mm^{-1})	0.643	0.298	0.770	0.619
Data, R_{merge}	6008, 0.0265	12633, 0.038	6359, 0.035	5671, 0.019
Unique data, $I > 2\sigma_I$	2984, 2076	4737, 4227	2422, 1758	3477, 2783
Completeness (%), max. θ (°)	96.4, 68.3	83.6, 24.3	99.5, 72.6	96.6, 72.4
R, wR (unique data)	0.078, 0.176	0.052, 0.104	0.065, 2422	0.060, 0.129
R ($I > 2\sigma_I$)	0.062	0.046	0.045	0.050
Parameters, restraints	219, 2	510, 7	174, 0	264, 70
Goodness-of-fit	1.075	1.015	1.006	1.027
Δρ(final) ($e^-/Å^3$)	+0.25, −0.22	+0.19, −0.16	+0.17, −0.16	+0.18, −0.14

Estimated standard deviations in parentheses. For (−)-**8**, absolute structure parameter −0.03 (9), extinction coefficient 0.0069(13), and major dithiolan ketal conformer: 0.52 (3). For (±)-**6b**, major side-chain butyl conformer [*anti*; torsion -162.3 (9)°] 0.613 (1), and minor [*gauche*, torsion −87.4 (6)°]. For (±)-**10**, major conformer 0.843 (4), extinction parameter 0.0039 (8)

donors and acceptors were displaced as required for ap-*syn-anti* configuration with (**a**: 20°, **b′**s: 0°, **d**: 0 pm, **Q** -19.1 pm) [7]. The $O{\cdot}O_{H\text{-}bond}$ was of ordinary length at 269 pm. In contrast, for 2-methyl-1,3-cyclohexandione enol, glide-related molecules showed arguably improved system alignment [8]. Hydrogen-bonded donors and acceptors adopted ap-*anti-anti* configuration, a π-system alignment described by **a**: 9°, **b**: 180°, **b′** 0°, **b″** 21°, **d**: 0 pm, and **Q** -17.2 pm, and a shorter 259 pm $O{\cdot}O_{H\text{-}bond}$ distance. This greater delocalization of the π-systems, and better alignment through the hydrogen-bonding were consistent with a RAHB effect [2].

Table 4 presents the alignment and delocalization data for the 4-hydroxycoumarin derivatives **2**–**11** studied here. Enolone alignment in these β-chains is linked to a maximal translational repeat distance of 717 pm along the interaction direction. Table 4 additionally reports on whether the β-chains of neighboring and interacting molecules have the same chirality (polar) or alternating chirality (non-polar), and the crystallographic relationship (pure translation, or glide) between relatives along the chain. In contrast, derivatives of 4-hydroxycoumarin without β-chains, **Q** is typically larger such as in a warfarin cyclic methyl ketal where it is 26 pm [44].

Phenprocoumon

Molecular packing and interactions in the crystal structures of (±)-**2** and (−)-**2a** are similar. Both structures form well-aligned translational β-chains with a 717 pm repeating unit, and the racemate shows polar β-chains, (S) with (S) and (R) with (R) [10, 12]. The dominant hydrogen-bonding patterns are infinite chains with motif $C_1^1(6)$ [45]. Since the spatial width of the side chain phenyl and ethyl groups are dimensionally smaller than the 4-hydroxycoumarin, the herringbone packing features in the layers perpendicular to the hydrogen-bonding direction leave considerable space for librational motions, more in the enantiomer which has a lower density and lower melting point than the racemate (vide supra and Table 1).

Table 4 Structural features for intermolecular H-bonding in selected chiral and racemic 3-substituted 4-hydroxycoumarins

Compound temp. (K)	Space group	H-bond axis, repeat (pm)	$O{\cdot}O_{H\text{-bond}}$ distance (pm)	Q (pm)	a (°)	b_{pitch}, b'_{roll}, b''_{yaw} (°, °, °)	d (pm)	β-chain type
β-Enolone hydrogen-bonding configuration: ap-*anti-anti*								
(±)-**2** [14] 295	P $2_1/n$	*c* 717.7	261.7	15.9	7.1	0, 0, 0	36	Transl., polar
(−)(S)-**2a** 298	P 2_1	*a* 717.2	260.6 262.7	17.0 16.9	6.6 7.4	0, 0, 0 0, 0, 0	15 43	Transl., polar
(−)(S)-**2b** 101	P 2_1	*a* 714.0	258.3 261.9	15.7 17.6	6.7 8.2	0, 0, 0 0, 0, 0	9 50	Transl., polar
(−)(S)-**8** 297	P 1	*a* 715.9	261.1 267.2	20.2 20.8	7.3 9.1	0, 0, 0 0, 0, 0	61 61	Transl., polar
(±)-**3** 297	P $2_1/a$	*a* 719.5	264.0	17.1	7.1	0, 0, 0	1	Transl., polar
(±)-**10** 298	P -1	*a* 717.2	262.6	18.3	7.2	0, 0, 0	23	Transl., polar
(−)-**3** 298 eutectic 72% (S)	P 2_1	*a* 716.4	264.1 262.6	23.8* 12.2* ‹18.0›	14.5 14.4	0, 0, 0 0, 0, 0	57 62	Transl. polar
(±)-**4** 297	P -1	*a* 2 (701.0)	268.2 269.4 270.4 271.4	17.5 17.8 18.4 19.0	12.1 12.7 13.7 14.1	−1, 22, 0 −1, 23, 0 	105 115 136 140	Transl., nonpolar
(±)-**11** [15] 298	P *bca*	*a* 2 (707.7)	266.0	16.0	12.5	180, 0, 10	80	Glide, polar
9 298	P $2_1/c$	*c* 2 (654.1)	270.9	18.1	19.5	60, 15, 15	186	Glide
β-Enolone hydrogen-bonding configuration: ap-*syn*-(*anti)*								
(±)-**6a** 101	P $2_1/c$	*c* 2 (617.8)	267.3	20.5	14.5	−117, 18, −30	173	Glide, nonpolar
(±)-**6b** 298	P $2_1/c$	*c* 2 (612.1)	267.9	20.7	15.7	−117, 18, −30	184	Glide, nonpolar
(±)-**5** 298	P $2_1/c$	*c* 2 (611.3)	269.6	20.6	16.6	−64, 21, −30	25	Glide, nonpolar
(±)-**7** [17] 293	C 2/*c*	*c* 2 (534.2)	270.2	19.5	18.4	−9, −56, 7	225	Glide, nonpolar

See text for term definitions

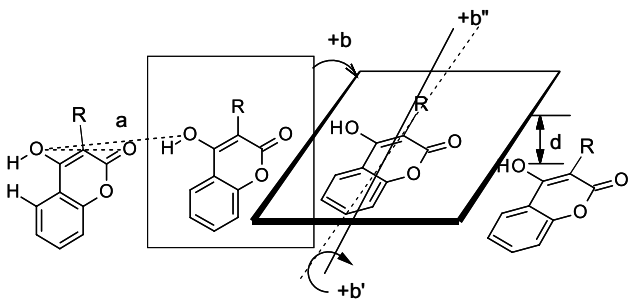

Fig. 3 Parameters for misalignment of translational 4-hydroxycoumarin β-ketoester enols illustrated for ap-*anti-anti* configuration

In racemic phenprocoumon, (±)-**2**, coumarins have ap-*anti-anti* configuration and hydroxys are hydrogen-bonded to lactone carbonyl oxygens in a translation neighbor with shortened $O{\cdot}O_{H\text{-bond}}$ 261.7 pm (Table 4) [10]. Oxygens are almost aligned with the crystallographic axis (**a**: 7.1°) with moderate delocalization in the β-ketoester enol (Q = 15.9 pm). Adjacent molecules also show C(5)–H···O,O′(ester) interactions supporting adjacent stronger O–H·O contacts. The C(–H)·O,O′ distances are 332 and 362 pm, and while longer and weaker than O–H·O contacts, nevertheless they are probably important as they occur nearly in the coumarin ring plane. Coumarins are stacked with π-system contacts at typical separations of 347 pm. But the narrower width of the phenyl ring (~400 pm) compared

to the coumarin system (715 pm) represents a size mismatch that permits looser packing and vibrational freedom for the side chain groups relative to the RAHB interactions that dominate the translational symmetry. The largest principal components of the atomic librations (U_{33}) are parallel to the RAHB direction along the *c*-axis (Fig. 4). The average U_{33} for the five enolone non-H atoms (along the β-chain) is 0.0378(3) Å^2, while the distal three carbons of the side-chain phenyl rings have average U_{33}'s nearly six times larger at 0.224(25) Å^2. The alternative explanation of a static disorder of side-chain groups seems less likely.

The crystal structure of the (−)(S)-**2a** (at 298 K) is similar to that of the racemate. The polar β-chains of (R)-enantiomers of the racemate are replaced with a second β-chain of (S)-enantiomers. For this study, we have re-determined (−)-(S)-**2a** because of the relatively large librations found in the original report [12]. Both independent β-chains have ap-*anti*-*anti* configurations related by translations along the *a*-axis with repeat distance 717.2 pm. Coumarins are oriented in opposing directions along the *a* axis in two polar strands, and delocalized enols were aligned for RAHB with **a**: 7°, **d**: 29 pm, Q = 17 pm in one strand, and **a**: 7°, **d**: 50 pm, Q = 17 pm in the other. The hydrogen-bonding schemes are the same as in the racemate with enolone hydrogen-bonds assisted by *peri C*–H interactions with the neighboring lactone oxygens. The O·O$_{H\text{-}bond}$ distances are shortened at 260.6 and 262.7 pm. As found in the racemate, librations of the distal side chain phenyl carbons are considerable (Fig. 5). The average U_{11} for the five enolone non-H atoms in each chain were 0.0308 (4) Å^2, and 0.0424 (29) Å^2, while the average U_{11} of the distal three carbons of the phenyl rings were at least four times larger at 0.210 (46) Å^2, and 0.164 (37) Å^2, respectively. Packing efficiency in the enantiomer (at 298 K, cell volume 1495.3 Å^3, mp 170–171 °C) was slightly less than in the racemate (at 295 K cell volume 1467.7 Å^3, mp 179–180 °C).

Often, large thermal motion occurs where crystal packing is in transition to a more stable form. On cooling crystals of (−)-(S)-phenprocoumon (**2a**) from 296 to 193 K, no evidence of a phase transition was detected by differential scanning calorimetry. When a crystal was cooled to 101 K, the diffraction pattern showed the same lattice as at room temperature. Cell volume was reduced to 1437.4 Å^3, most of which resulted from reduction in the cell repeats orthogonal to the axial hydrogen-bonding direction. The β-chain O·O$_{H\text{-}bond}$'s were only reduced slightly to 258.3 pm and 261.9 pm, respectively (Table 2). The average U_{11} for the five enolone non-H atoms in each chain were 0.0116 (18) Å^2, and 0.0252 (40) Å^2, while the average U_{11} of the distal three carbons of the phenyl rings were still at least twice as large at 0.119 (37) Å^2, and 0.054 (15) Å^2, respectively, at this lower temperature.

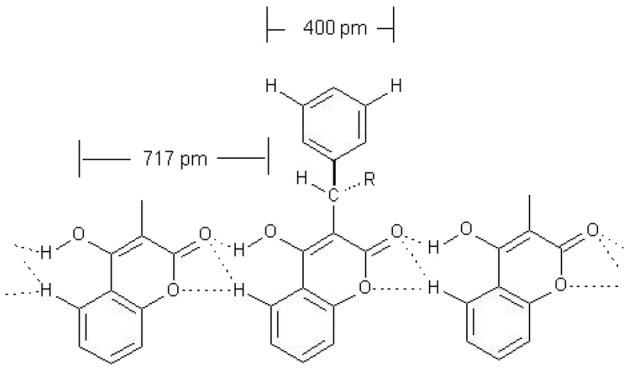

Fig. 4 Side-chain phenyl groups are not as wide as 4-hydroxycoumarins allowing ap-*anti*-*anti* β-chains. [R = methyl (**3**), ethyl (**2**), *i*-propyl (**4**), 2′,2′-ethandithioprop-1′-yl (**8**), 2′,2′-dimethylprop1′-yl (**10**)]

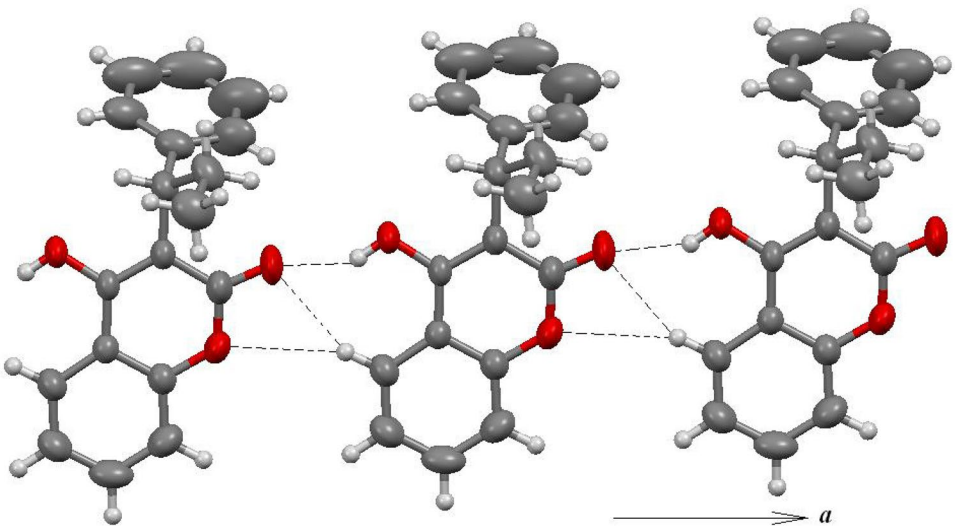

Fig. 5 Translational hydrogen-bonding in one of the two polar chains of (−)(S)-phenprocoumon (**2a**) at 298 K showing ap-*anti*-*anti* configuration and the considerable librations in the side chains

Other Coumarins

Translational Chains

The structures of (±)-**3**, (−)-**3**, (±)-**4**, (−)-**8, 9** and (±)-**10** all show translational β-chains and ap-*anti-anti* configurations of their enolones. In structure (±)-**3**, polar translational β-chains are present with repeat distance 720 pm and O·$O_{H\text{-}bond}$'s of 264 pm. Compound **3** was partially resolved with (+)-quinidine and after isolation, recrystallization did not improve the enantiomeric enrichment beyond a putative eutectic composition. This partially resolved phase is chiral and it is styled here as (−)-**3**, and crystals occur in the non-centrosymmetric space group $P2_1$ with repeat distance 716 pm. The structure shows two inequivalent polar translational β-chains, one ordered with (S)-enantiomers. The second β-chain is also polar but with (S)-isomer occupancy 0.215 (1), and therefore this phase is 60.7% (S) and 39.3% (R). In the second chain, librations are greater for the side chain atoms of the (S) molecule compared those of the (R), suggesting that the side chains of the (S)-isomers are less tightly packed. A similar disparity in packing efficiency and in librational freedom was observed between the racemate and enantiomeric phases of **2** (vide supra). Apparent overlap of the side chain phenyl and methyl groups was modeled with the help of restraints during refinement. But the overlap of the coumarins was essentially perfect within the resolution of the determination. This was consistent with the importance of the hydrogen-bonded β-enolone interactions in the organization of the structure. The bond metrics for (−)-**3** are however less accurate; the average Q is 18 and coumarins are well aligned with slightly shorter O·$O_{H\text{-}bond}$ contacts and a modest claim for RAHB. Coumarins of (−)-**3** are stacked with weak contacts between their parallel but offset π-systems, and ring separations of about 350 pm.

In the chiral structure (S)-(−)-**8**, space group P 1, there are two independent molecules in the asymmetric unit each of which form (polar) translational β-chains with good alignment of the enolones. Acceptor oxygens are displaced by 61 pm from the donor enolone plane but otherwise the chains are well aligned and consistent with the 716 pm repeat, and 264 pm average O·$O_{H\text{-}bond}$ distance. Coumarins of (S)-(−)-**8** are stacked with weak contacts between their parallel but offset π-systems, and ring separations of about 350 pm. This structure shows disorder between conformations of the dithioketal ethylene bridge which acts to reduce the accuracy in its bond metrics.

The structure of (±)-**4** shows four independent molecules in the asymmetric unit, with two non-polar translational β-chains linking (R) with (S) along the (2 × 702) pm *a*-axis. This structure shows non-crystallographic (1/2 + x, y, z) symmetry along the β-chain direction which was satisfactorily modeled. The lattice is triclinic, space group P -1, with $a \approx c$, and $\gamma \approx 90.0°$. Alignment of the coumarins is poorer than in **2** or **3**, for example (Table 4), with **a** about 12–14°, the β-chains were slightly corrugated by a molecular roll (**b'** about 22°) and the O·$O_{H\text{-}bond}$'s are on average longer (272 pm) than in **2** and **3**. The shorter semi-repeat was consistent with the misalignment. Coumarins of **4** are stacked with weak contacts between their π-systems with parallel pairs alternating with pairs 10.9° from parallel, and ring separations of about 370 and 365 pm, respectively.

In one of two structures taken from the literature, 3-(1′-naphthyl)-4-hydroxycoumarin, **(±)-11**, translational β-chains were polar with the molecules showing axial (substituted biphenyl-like) chirality [15]. Molecules were related by a crystallographic glide (180° pitch angle **b**) along the β-chains. The β-enolones had ap-*anti-anti* configuration, as with the other polar chain structures, but enolone alignment was poorer. Modest molecular yaw (**b″** 10°) was consistent with a slightly shortened 708 pm semi-repeat, and the slightly longer 266 pm O·$O_{H\text{-}bond}$ distance. This structure showed that a glide relationship between hydrogen-bonded 4-hydroxycoumarins still employed the ap-*anti-anti* configuration like that in Fig. 5. Coumarins in **11** were stacked parallel but offset, and with an interplanar spacing of about 365 pm. More typically in the group studied, racemic structures had non-polar enolone chains with glide relations.

Transitional Structures

Structures **4** and **9** form a transitional group between structures with the polar (translation) and non-polar (glide) β-enolone hydrogen-bonded chains, but retaining ap-*anti-anti* configurations. Modest molecular misalignments between enolones are accompanied by slightly shorter crystallographic repeating distances along the enolone chain (Table 4).

Glide Related Chains

Compounds **5**, **6** and **7** all have longer side chains on the 3-substituent carbon. These racemates each show non-polar β-chains with hydrogen-bonding between glide relatives, and ap-*syn*-(*anti)* configurations in contrast to structures of **2**–**4**, **8**, **9**. Structures **5**–**7** show considerable misalignments (higher **a** and **b** values), less enolone delocalization (higher **Q** values), weaker hydrogen-bonding (averaging O·$O_{H\text{-}bond}$ 269 pm), and modest molecular roll and yaw resulting in corrugated coumarin arrangements with significantly shorter β-chain repeat distances (Table 4). These glide-related β-chains were also influenced by temperature change. While the fully-extended form represented by structures **2a** and **2b**

showed contraction of the cell and the $O{\cdot}O_{Hbond}$ distance along the translational hydrogen-bonding direction on cooling (from 298 to 101 K), compound **6** showed a lengthening along the β-enolone repeat direction and a very small reduction in the $O{\cdot}O_{Hbond}$ contact distance on cooling. The β-chain is illustrated for structure **6b** in Fig. 6. Coumarins of **5**, **6**, **7** are stacked with weak contacts between their parallel but offset π-systems, and ring separations of about 350 pm, 345 pm, and 345 pm respectively.

General Comments

The polar translational β-chains are sufficiently stabilizing in structures with smaller 3-substituents to allow excellent alignment of the coumarins (**2**, **2a**, **2b**, **8**, **3**) which are supported by ap-*anti*-*anti* enolone configurations. Delocalization Q's (about 15) and O–H·O s (about 260 pm) are consistent with previous observations on RAHB systems [10]. In the enantiomeric phases (**2a**, **2b**, **8**, **3**), one of the two polar chains has just slightly stronger hydrogen-bonding. The racemates studied (**2**, **3**) have slightly higher densities and better packing, retaining the polar β-enolone structure. Where substituents begin to affect the alignment of the β-enolones, modest molecular roll and yaw (corrugated arrangements) and a doubling of the molecular repeat continue to accommodate the translational associations, but with weaker hydrogen-bonding and poorer π-alignment (**4**, **9**). For some larger or longer substituents, pure translational β-enolones are replaced with non-polar glide relations with required doubling of the molecular repeats (typically observed along a crystallographic axis). Alignments now show a general freedom with accommodating molecular pitch, yaw and roll, ap-*syn*-(*anti*) enolone structure, loss of buttressing C–H·O contacts, weaker hydrogen-bonding, and contracting crystallographic repeat distances. Coumarin ring π-stacking, typically with parallel arrangements and offsets, but occasionally at a shallow angle, are common features of the entire group.

Testing the General Trends

Structures **9** and **10** were examined to test some of the β-enolone interaction features just recited and learned from structures **2**–**8**, **11**. It seems that longer unbranched R groups (Fig. 4) eventually lead to weakened β-chains. To gauge this in an approximate way, we examined the structure of 3-benzyl-4-hydroxycoumarin (**9**) in which the side-chain is now H, and a longer branched chain derivative **10**. Achiral **9** forms hydrogen-bonded β-chains between glide relatives along the hydrogen-bonding direction (*c* axis in P $2_1/c$) and uses ap-*anti*-*anti* configuration and an intermediate semi-repeat of 645 pm (Table 4). Delocalization of the π-system is poorer (Q 19.5), and the hydrogen-bond length is of the weaker variety at 270 pm. For compound racemic **10**, well-aligned polar β-chains between enolones are found as with the examples with shorter side chains (Table 4) and also the longer branched chain structure (S)-(−)-**8**. Coumarin rings show π-stacking with parallel arrangements, and with interplanar separations of 348 pm in **9**, and 355 pm in **10**.

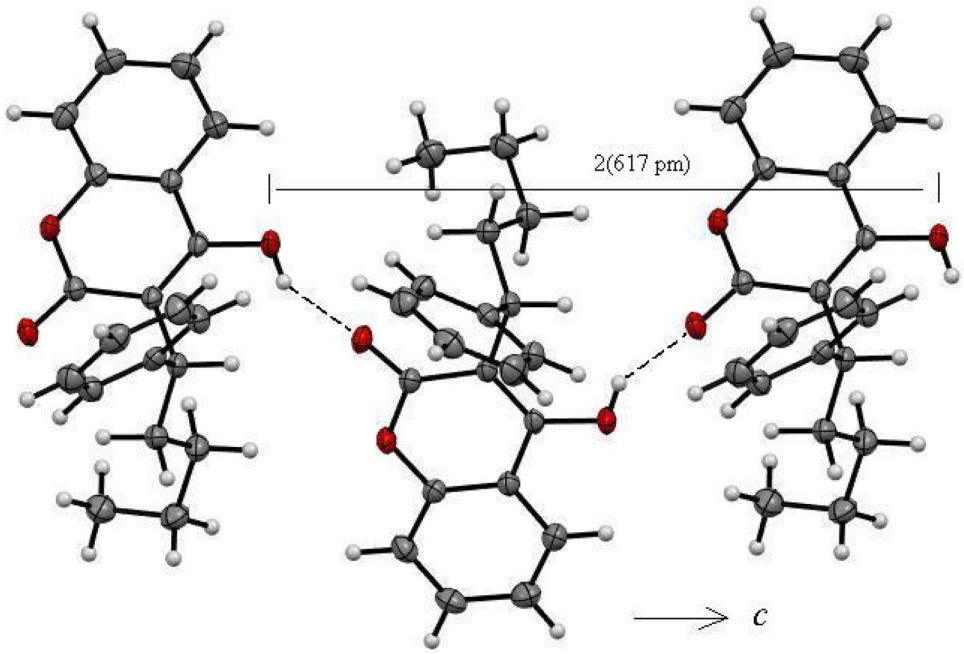

Fig. 6 Hydrogen-bonds between glide relatives in the non-polar β-chains of structure (±)-**6a**, and showing ap-*syn*-(*anti*) enolone configuration

Conclusions

3-Substituted-4-hydroxycoumarins without competing hydrogen-bonding interactors show tendencies toward β-chain formation. The structures examined here are related more or less closely to phenprocoumon (**2**), a compound with a benzylic chiral center attached at the 3-position of 4-hydroxycoumarin. For shorter side-chains or longer branched side-chains on the benzylic chiral carbon, enolones align well for ap-*anti-anti* configurations, show modest π-delocalization, a translational repeat distance of about 717 pm, and somewhat stronger hydrogen-bonding with $O{\cdot}O_{H\text{-}bond}$ distances below about 265 pm. These features are consistent with resonance-assisted hydrogen-bonding (RAHB). For longer straight-chain benzylic substituents, non-polar β-chains are found between glide relatives with poorly aligned enolones and using ap-*syn*-(*anti*) configurations, necessarily poorer π-delocalization, and hydrogen-bonding $O{\cdot}O_{H\text{-}bond}$ distances above 265 pm. Crystallographic semi-repeat distances are shorter than for the better aligned groups. Still other structures that may be considered intermediate between these two groups have also been found which retain ap-*anti-anti* configurations, either translational or glide relatives, but with considerably diminished system alignment and weaker hydrogen-bonding. Generally, coumarins show π-stacking with interring distances of about 355 pm.

Acknowledgements EJV thanks the National Science Foundation (MRI-0618148) for support of crystallographic equipment. Thanks also go to Dr. Verner Schomaker (deceased) of the University of Washington for his encouragement, acumen, persistence and pedagogy with difficult structures.

Compliance with Ethical Standards

Conflict of interest All the authors declare no conflict of interest.

References

1. Steed JW, Turner DR, Wallace KJ (2007) Core concepts in supramolecular chemistry and nanochemistry. Wiley, Chichester
2. Gilli G, Bellucci F, Ferretti V, Bertolasi V (1989) Evidence for resonance-assisted hydrogen bonding from crystal-structure correlations on the enol form of the β-diketone fragment. J Am Chem Soc 111:1023–1028
3. Bertolasi V, Gilli P, Ferretti V, Gilli G (1996) Resonance-assisted O-H…O hydrogen bonding: its role in the crystalline self-recognition of β-diketone enols and its structural and IR characterization. Chem Eur J 2(8):925–934
4. Sanz P, Mo O, Yanez M, Elguero J (2007) Resonance-assisted hydrogen bonds: a critical examination. structure and stability of the enols of β-diketones and β-enaminones. J Phys Chem 111:3585–3591
5. Gora RW, Maj M, Grabowski SJ (2013) Resonance-assisted hydrogen bonds revisited Resonance stabilization vs. charge delocalization. Phys Chem Chem Phys 15:2514–2522
6. Gilli P, Pretto L, Bertolasi V, Gilli G (2009) Predicting hydrogen-bond strengths from acid-base molecular properties the pK_a slide rule: toward the solution of a long-lasting problem. Acc Chem Res 42(1):33–44
7. Tadeusz M, Krygowski J, Zachara-Horeglad E (2009) Resonance-assisted hydrogen bonding in terms of substituent effect. Tetrahedron 65:2010–2014
8. Beck JF, Mo Y (2007) How resonance assists hydrogen bonding interactions: an energy decomposition analysis. J Comput Chem 28:455–466
9. Grabowski JS (2009) Covalent character of hydrogen bonds enhanced by π-electron delocalization. Croat Chem Acta 82:185–192
10. Gilli G Bertolasi, Feretti V, Gilli P (1993) Resonance assisted hydrogen bond. III. Formation of intermolecular hydrogen-bonded chains in crystals of β-diketones and its relevance to molecular association. Acta Crystallogr B49:564–576
11. Trifonov L, Bieri JH, Prewo R, Dreiding AS, Rast DM, Hoesch L (1982) The constitution of veretinolide, a new derivative of tetronic acid, Produced by Verticillium Intertextum. Tetrahedron 38(3):397–403
12. Katrusiak A (1993) Structure of 2-methyl-1,3-cyclohexandione crystals. J Crystallogr Spectrosc Res 23(5):367–372
13. Gaultier J, Hauw C (1966) Structure del'hydroxy-4-coumarine. Eau d'Hydroation et Cohesion Cristalline. Acta Crystallogr 20:646–651
14. Bravic G, Gaultier J, Hauw C (1971) Structure cristalline et moleculaire du marcoumar. C R Acad Sci Paris C272:1112–1114
15. Bravic G, Gaultier J, Geoffre S, Hauw C (1974) Structure crystalline d'une antivitamine K: 1'α-naphthyl-3-hydroxy-4-coumarine. C R Acad Sci Paris 278:601–603
16. Valente EJ, Trager WF, Lingafelter EC (1976) (–)–3–(1–Phenylpropyl)–4–hydroxycoumarin. Acta Crystallogr B32:277–279
17. Manolov I, Maichle-Moessmer C (2007) Crystal structure of 4-hydroxy-3-[1-phenyl-2-(4-methoxybenzoyl)ethyl]-2H-1-benzopyran-2-one. Anal Sci 23:X79 **(See CCDC 637813)**
18. Bravic G, Gaultier J, Hauw C (1968) Structure crystalline et moleculaire du dicoumarol. C R Acad Sci Paris 267:1790–1795
19. Alcock NW, Hough E (1972) The crystals and molecular structure of 3,3-methylene(bis-6-bromo-4-hydroxycoumarin): unusual molecular interactions. Acta Crystallogr B28:1957–1960
20. Valente EJ, Eggleston DS (1989) Structure of (phenyl)bis(4-hydroxybenzo-2H-pyran-2-one-3-yl)methane. Acta Crystallogr C45:785–787
21. Stancheva S, Maichle-Mössmerb C, Manolova I (2007) Synthesis, structure and acid-base behaviour of some 4-hydroxycoumarin derivatives. Zeitschrift fur Naturforschung 62:737–741
22. Ravikumar N, Gopikrishna G, Solomon KA (2012) 3,3'-[(4-Nitrophenyl)methylene]-bis(4-hydroxy-2H-chromen-2-one). Acta Crystallogr E 68:o265
23. Li M-K, Li J, Liu B-H, Zhou Y, Li X, Xue X-Y, Hou Z, Luo X-X (2013) Synthesis, crystal structures, and anti-drug-resistant *Staphylococcus aureus* activities of novel 4-hydroxycoumarin derivatives. Eur J Pharmacol 721:151–157
24. Chang-Wei LV, Yao-Ping WU, Jian L, Xin-Gang J (2012) 3,3'-(4-Dimethylamino benzylidene)-bis-(4-hydroxycoumarin). Chin J Struct Chem 31:847–850
25. Manolol I, Ströebele M, Meyer H-J (2008) Crystal structure of 4-hydroxy-3-[(2-oxo-2H-chromen-3-yl)-(3,4,5-trimethoxyphenyl) methyl]chromen-2-one. Anal Sci 24:x135–x136
26. Manolov I, Morgenstern B, Hegetschweiler K (2012) Synthesis and structure of ethyl 2-[bis(4-hydroxy-2-oxo-2H-chromen-3-yl) methyl]benzoate. X-Ray Struct Anal Online 28:83–84

27. Manolov I, Morgenstern B, Hegetschweiler K (2012) Synthesis and Structure of 4-Hydroxy-3-[(2-oxo-2H-chromen-3-yl)-3,4-dihydroxyphenyl)methyl]chromen-2-one ethanol solvate. X-Ray Struct Anal Online 28:87–88
28. Manolov I, Maichle-Moessmer C (2013) Synthesis and crystal structure of 4-hydroxy-3-[(3E)-3-(hydroxyimino)-1-(4-nitrophenyl)butyl]-2H-chromen-2-one. Bulg Chem Commun 45(1):109–113
29. Asas M, Oo C-W, Osman H, Quah CK, Fun H-K (2010) 3-[(E)-3-(2,4-Dichloro phenyl)prop-2-enoyl]-4-hydroxy-2H-chromen-2-one. Acta Crystallogr 66E:o3022–o3023
30. Naveen S, Adlakha P, Upadhyay K, Shah A, Anandalwar SM, Prasad JS (2006) Crystal structure of 3-nitro-4-hydroxycoumarin. Anal Sci 22:x103–x104
31. Stefanou V, Matiadis D, Melagraki G, Afantitis A, Athanasellis G, Igglessi-Markopoulou O, McKee V, Markopoulos J (2011) Functionalized 4-hydroxycoumarins: novel synthesis, crystal structure and DFT calculations. Molecules 16:384–402
32. Pohl LR, Haddock R, Garland WA, Trager WF (1975) Synthesis and thin-layer chromatographic, ultraviolet, and mass spectral properties of the anticoagulant phenprocoumon and its monohydroxylated derivatives. J Med Chem 18(5):513–519
33. West BD, Link KP (1965) The resolution and absolute configuration of marcumar. J Heterocycl Chem 2(1):93–94
34. Kischel J, Mertins K, Michalik D, Zapf A, Bellera M (2007) A general and efficient iron-catalyzed benzylation of 1,3-dicarbonyl compounds. Adv Synth Catal 2007(349):865–870
35. Theerthagiri P, Lalitha A (2010) Benzylation of β-dicarbonyl compounds and 4-hydroxycoumarin using TMSOTf catalyst: a simple, mild, and efficient method. Tetrahedron 51:5454–5458
36. West BD, Preis S, Schroeder CH, Link KP (1961) Studies on 4-hydroxycoumarins. XVII. The resolution and absolute configuration of warfarin. J Am Chem Soc 83(12):2676–2679
37. Liu Z-Q, Zhang Y, Zhao L, Li Z, Wang J, Li H, Wu L-M (2011) Iron-Ctalyzed stereospecific olefin synthesis by direct coupling of alcohols and alkenes with alcohols. Org Lett 13(9):2208–2211
38. Appendino G, Cravotto G, Tagliapietra S, Ferraro S, Nano GM (1991) The chemistry of coumarin derivatives. Part 3. Synthesis of 3-alkyl-4-hydroxycoumarins by reductive fragmentation of 3,3'-alkylidine-4,4'-dihydroxybis[coumarins]. Helv Chim Acta 74:1451–1458
39. Stahmann MA, Wolff I, Link KP (1943) Studies on 4-hydroxycoumarins. I. The synthesis of 4-hydroxycoumarins. J Am Chem Soc 65:2285–2287
40. Clark RS, Reid JS (1995) The analytical calculation of absorption in multifaceted crystals. Acta Crystallogr A51:887–897
41. Sheldrick GM (2008) A short history of SHELX. Acta Crystallogr A64:112–122 (recent program release from 2018)
42. Mercury (2016) version 3.9, Cambridge Crystallographic Data Center
43. Steiner T (2002) The hydrogen bond in the solid state. Angew Chem Int Ed 41:48–76
44. Valente EJ, Eggleston DS, Schomaker V (1986) Structures of Five *trans*–2–hydroxy and methoxy–2–methyl–3,4–dihydro–4-aryl–2H,5H–pyrano [3,2–c] [1]benzopyran–5–ones. Acta Crystallogr A C42:1809–1813
45. Etter MC, MacDonald JC, Bernstein J (1990) Graph-set analysis of hydrogen-bond patterns in organic crystals. Acta Crystallogr A B46:256–262

Publisher's Note Springer Nature remains neutral with regard to jurisdictional claims in published maps and institutional affiliations.